

pubs.acs.org/JACS Communication

Sequential Modifications of Metal—Organic Layer Nodes for Highly Efficient Photocatalyzed Hydrogen Atom Transfer

Haifeng Zheng, Yingjie Fan, Abigail L. Blenko, and Wenbin Lin*



Cite This: J. Am. Chem. Soc. 2023, 145, 9994–10000



ACCESS I

III Metrics & More

Article Recommendations

Supporting Information

ABSTRACT: Herein, we report the synthesis of a bifunctional photocatalyst, Zr-OTf-EY, through sequential modifications of metal cluster nodes in a metal—organic layer (MOL). With eosin Y and strong Lewis acids on the nodes, Zr-OTf-EY catalyzes cross-coupling reactions between various C—H compounds and electron-deficient alkenes or azodicarboxylate to afford C—C and C—N coupling products, with turnover numbers of up to 1980. In Zr-OTf-EY-catalyzed reactions, Lewis acid sites bind the alkenes or azodicarboxylate to increase their local concentrations and electron deficiency for enhanced radical additions, while EY is stabilized by site isolation on the MOL to afford a long-lived catalyst for hydrogen atom transfer. The proximity between photostable EY sites and Lewis acids on the nodes of Zr-OTf-EY enhances the catalytic efficiency by approximately 400 times over the homogeneous counterpart in the cross-coupling reactions.

irected photocatalyzed hydrogen atom transfer (HAT) is widely used in the transformation of aliphatic C-H bonds into C-C, C-N, C-O, C-F, and C-S bonds. In these reactions, a photocatalyst uses photon energy to trigger the homolytic cleavage of C-H bonds in organic compounds to generate open-shell R· species for further transformations (Figure 1a). 1-4 The ability of aromatic ketones to abstract a hydrogen atom has been known since the birth of photochemistry, and these carbonyl derivatives have gained much attention as HAT catalysts in the recent renaissance of photochemistry and photocatalysis. 4-10 Upon irradiation, the long-lived triplet state of a carbonyl compound can abstract hydrogen from an aliphatic C–H compound to initiate radical-based coupling reactions. ^{11–14} For example, HAT catalysts and Lewis acids can synergistically mediate hydrofunctionalization of electron-deficient alkenes. 15-17 Lewis acids activate alkenes for the addition of radicals which are generated from a photoinduced HAT process.

The catalytic efficiency of hydrofunctionalization reactions is, however, limited by deactivation of photocatalysts via radical dimerization or radical trapping. A high catalyst loading (above 10 mol %) is typically needed to generate hydrofunctionalization products in moderate yields. It is highly desirable to develop bifunctional catalytic systems that synergize Lewis acids and photocatalysts for efficient hydrofunctionalization of olefins.

Metal—organic frameworks (MOFs) have provided a versatile platform for studying single-site catalysis and the synergy between multiple functionalities.^{21–24} MOFs isolate catalytic centers to prevent catalyst deactivation via multimolecular decomposition processes. Recently, Duan and coworkers encapsulated anthraquinone into MOFs to obtain a site-isolated HAT photocatalyst, which accelerates reverse HAT and prevents catalyst decomposition via dimerization.²⁵ However, the three-dimensional structures of MOFs cannot readily accommodate hierarchical installation of multiple active

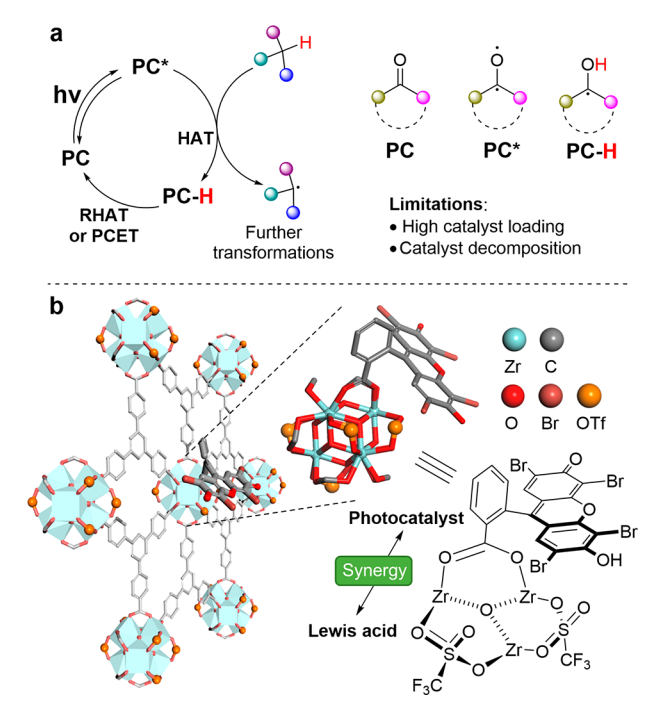


Figure 1. (a) Directed photocatalyzed hydrogen atom transfer (HAT) by carbonyl-based photocatalysts. (b) Schematic showing the design of a MOL-based bifunctional HAT photocatalyst for sustainable photocatalysis.

Received: March 14, 2023 Published: May 1, 2023





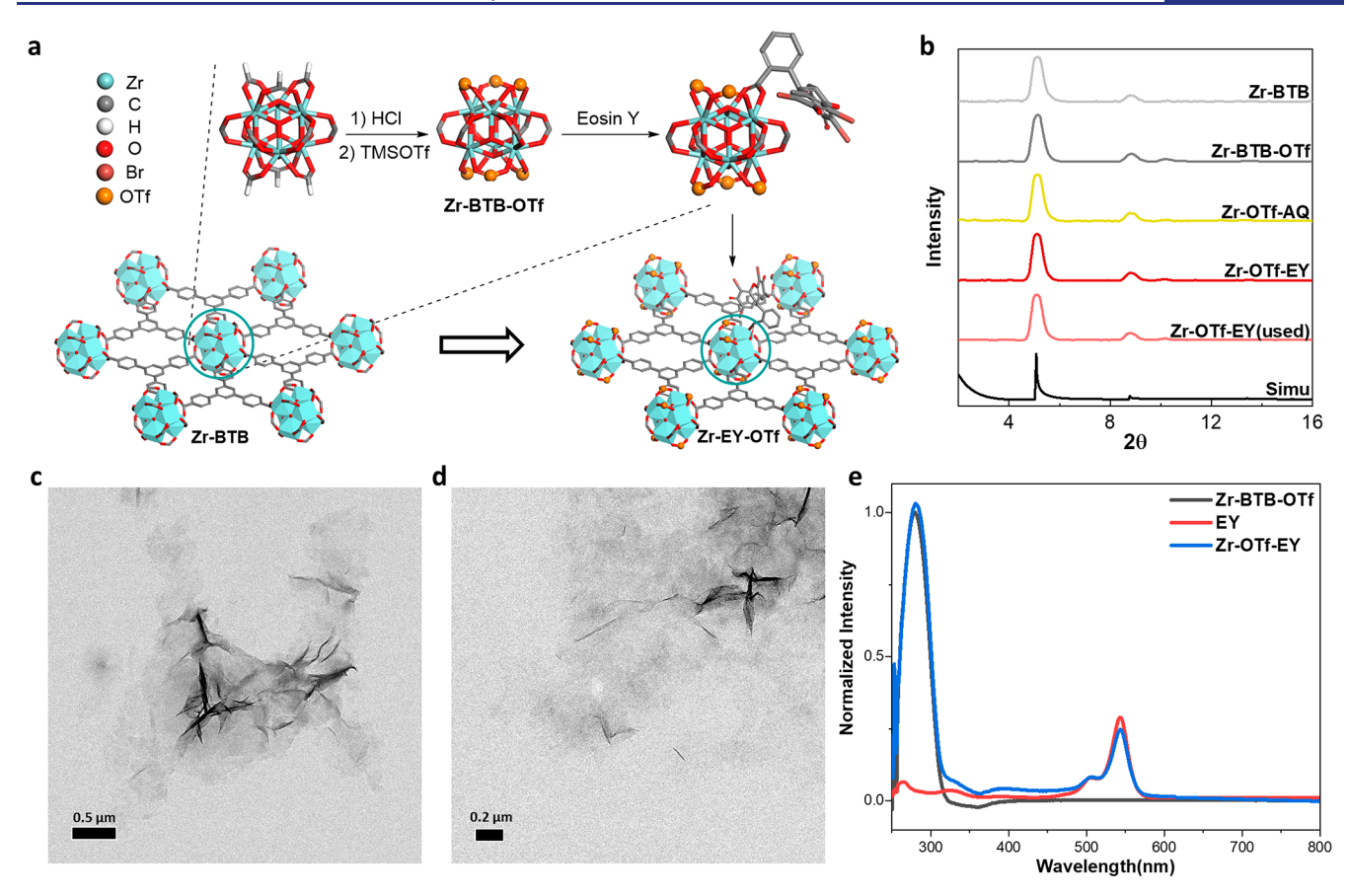


Figure 2. Synthesis and characterization of Zr-OTf-EY. (a) Scheme showing the synthesis of Zr-OTf-EY. (b) PXRD patterns of Zr-BTB, Zr-BTB-OTf, Zr-OTf-AQ, and Zr-OTf-EY before and after the catalytic reaction, along with the simulated PXRD pattern for Zr-BTB. (c, d) TEM images of Zr-BTB-OTf and Zr-OTf-EY. (e) UV—vis spectra of digested Zr-BTB-OTf, EY, and digested Zr-BTB-EY.

sites.^{26–33} We have developed two-dimensional metal—organic layers (MOLs) via proximal installation of multiple functionalities to promote synergistic and tandem photoredox catalysis.^{34–39} We hypothesized that a bifunctional HAT photocatalyst could be synthesized by installing Lewis acids and HAT photocatalysts through sequential modifications of secondary building units (SBUs) or nodes (Figure 1b).⁴⁰ We further posited that the proximally placed Lewis acids and HAT catalysts could synergistically activate olefinic substrates for the addition of HAT-generated radicals to accelerate reaction rates and improve selectivity for hydrofunctionalization products.

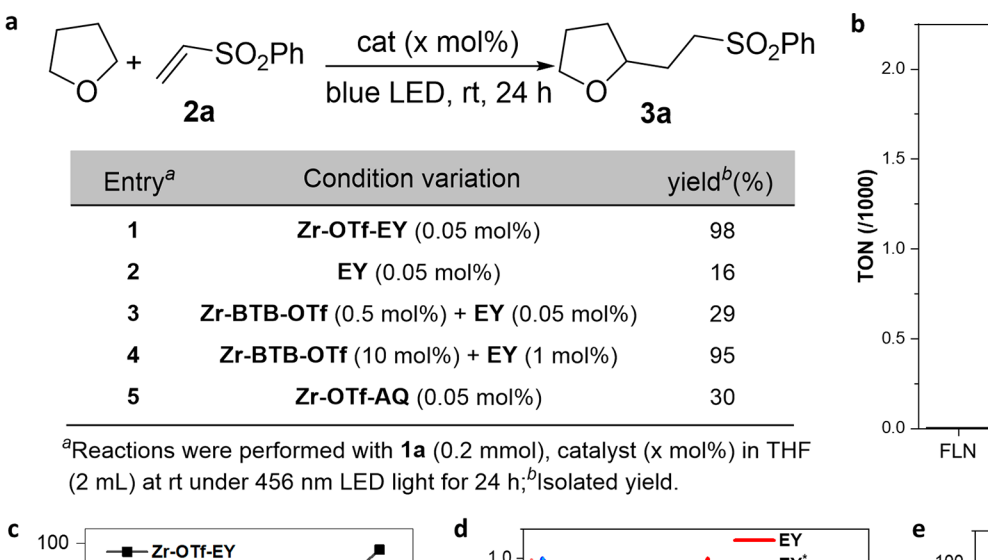
In this work, we synthesized a new Zr-OTf-EY MOL containing strongly Lewis acidic triflate-modified Zr_6 -SBUs and eosin Y (EY) photosensitizers for photocatalyzed HAT reactions. The Zr_6 SBUs of Zr-BTB MOL (BTB = 4-[3,5-bis(4-carboxyphenyl)phenyl]benzoate) underwent sequential modifications to generate Zr-triflate moieties and install EY photosensitizers. The resultant Zr-OTf-EY efficiently catalyzed HAT cross-coupling reactions of electron-deficient alkenes and azodicarboxylate with C–H compounds, with turnover numbers (TONs) of up to 1980 and a 400-fold higher catalytic efficiency over the homogeneous control.

A solvothermal reaction between $ZrCl_4$ and H_3BTB in N,N-dimethylformamide (DMF) with formic acid and water at 120 °C afforded the known Zr-BTB MOL with a formula of $Zr_6(\mu_3$ -O) $_4(\mu_3$ -OH) $_4(BTB)_2(HCO_2)_6$ (Figure 2a). In Zr-BTB, the Zr_6 SBUs are laterally bridged by BTB ligands and vertically terminated by formate groups to afford an infinite 2D

network. Zr-BTB was then treated with 1 M HCl to transform the terminating Zr₂-formate into Zr₂-OH/OH₂. 38,44 Subsequent triflation by trimethylsilyl triflate produced strongly Lewis acidic Zr₂-OTf sites on the SBUs. 38 Reaction of Zr-BTB-OTf with EY in acetonitrile at 60 °C yielded Zr-OTf-EY by partially replacing OTf capping groups with the carboxylates in EY (Figure 2a). 1 H NMR analysis of the digested Zr-OTf-EY gave an EY to BTB molar ratio of 0.1:1 (Figures S7, S8). Another HAT photocatalyst, 4-(9,10-dioxo-9,10-dihydroan-thracen-2-yl)benzoic acid (AQ), was similarly loaded on Zr-BTB-OTf to afford a bifunctional Zr-OTf-AQ HAT photocatalyst.

Zr-BTB, Zr-BTB-OTf, Zr-OTf-AQ, and Zr-OTf-EY showed similar powder X-ray diffraction (PXRD) patterns that matched the simulated pattern for Zr-BTB (Figure 2b), demonstrating the preservation of the 2D network structure upon SBU modifications. Transmission electron microscopy (TEM) showed ruffled nanosheet morphologies for Zr-BTB-OTf and Zr-OTf-EY (Figure 2c,d), whereas the UV-vis spectrum of digested Zr-OTf-EY showed contributions from both BTB ligand and EY.

Zr-OTf-EY was examined as a bifunctional HAT photocatalyst for the cross-coupling reaction between tetrahydrofuran (THF) and phenyl vinyl sulfone (2a). At 0.05 mol % loading of Zr-OTf-EY, the addition product 3a was obtained in 98% yield with a 1960 TON under blue LED irradiation (Figure 3a, entry 1). In comparison, a mixture of 0.05 mol % EY and 0.5 mol % Zr-BTB-OTf produced 3a in 29% yield (Figure 3a, entry 2). The yield of 3a further decreased to 16%



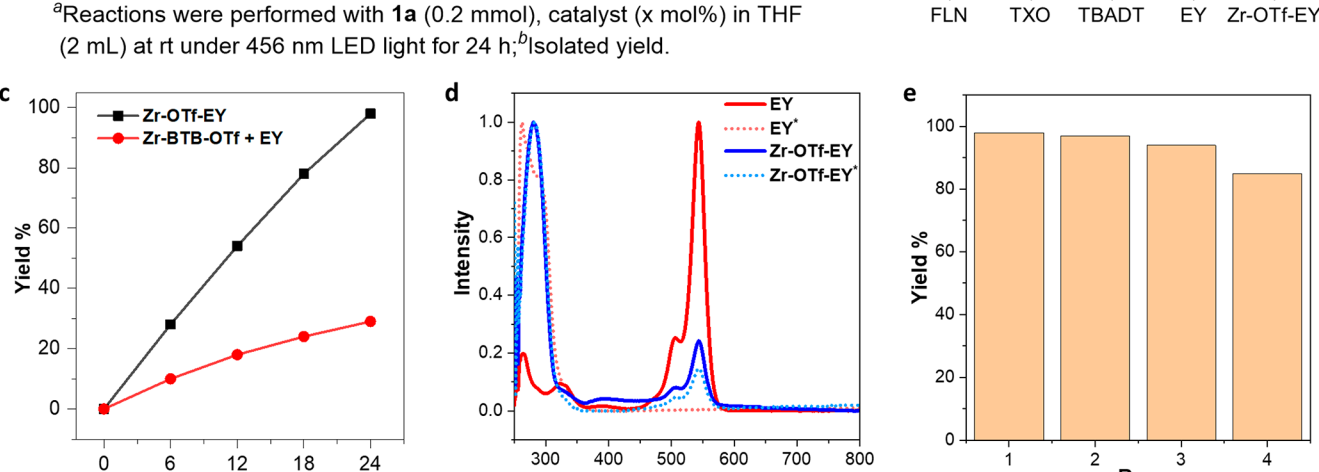


Figure 3. (a) Cross-coupling reactions between THF and 2a catalyzed by Zr-OTf-EY and control groups. (b) TONs of Zr-OTf-EY and other HAT catalysts. (c) Time-dependent conversions for the reactions catalyzed by 0.05 mol % Zr-OTf-EY or 0.05 mol % EY and 0.5 mol % Zr-BTB-OTf. (d) UV—vis spectra of EY and Zr-OTf-EY before and after the coupling reactions. UV—vis spectra after reactions were labeled with *. (e) Yields of 3a in four consecutive runs of Zr-OTf-EY-catalyzed coupling reactions.

Wavelength (nm)

in the presence of 0.05 mol % EY (Figure 3a, entry 3), indicating an important role of the Lewis acid in the reaction. Approximately 20-fold higher loadings of both Zr-BTB-OTf and EY were needed to afford 3a in a yield comparable to that of Zr-OTf-EY (Figure 3a, entry 4), suggesting approximately 400-fold higher catalytic efficiency for Zr-OTf-EY over the homogeneous control. Zr-OTf-AQ MOL showed lower activity and afforded 3a in 30% yield (Figure 3a, entry 5). Additionally, in the cross-coupling between THF and 2a, Zr-OTf-EY exhibited orders of magnitude higher TONs than other commonly used HAT catalysts, including 9-fluorenone (FLN), thioxanthone (TXO), and tetrabutylammonium decatungstate (TBADT) with TONs of 3.6, 4.6, and 45, respectively (Figure 3b). Time-dependent experiments were also performed for coupling reactions between THF and 2a, using 0.05 mol % Zr-OTf-EY or 0.05 mol % EY and 0.5 mol % Zr-BTB-OTf as catalysts under identical conditions (Figure 3c). Zr-OTf-EY catalyzed the reaction about three times faster than the homogeneous control. These results suggest a strong synergy between the HAT photocatalyst and the Lewis acid in Zr-OTf-EY due to the proximity between catalytic sites on the MOL.36,39

Time (h)

Zr-OTf-EY remained stable under photocatalytic conditions, as evidenced by the retention of the PXRD pattern and UV—vis spectrum for the recovered catalyst (Figures 2b, 3d). However, UV—vis spectroscopy revealed the decomposition of

EY under photocatalytic conditions in the homogeneously catalyzed reaction (Figure 3d). After 24 h of irradiation, the characteristic peak of EY at 543 nm completely disappeared with the appearance of new peaks below 300 nm. Zr-OTf-EY was also recovered and reused in four runs of cross-coupling reactions between THF and 2a without a significant decrease in catalytic activity (Figure 3e).

Run

The Lewis acidity of Zr-OTf-EY was quantified using Nmethylacridone (NMA) as a fluorescence probe. 49 The emission peak maxima of NMA shift to longer wavelengths when bound to Lewis acids. The differences are used to qualitatively compare the Lewis acidity of different acids. Zr-OTf-EY and TiCl₄ shifted NMA emission peak maxima from 413 nm to 472 and 474 nm, respectively, indicating their similar Lewis acidity (Figure S12b). The activation of 2a by TiCl₄ was further confirmed by ¹H NMR (Figure S12c). Proton signals of 2a all shifted to lower field upon addition of TiCl₄ to a solution of 2a. The proton at the anti-position to the sulfone group shifted the most, from 6.04 ppm to 6.31 ppm, indicating the binding of sulfone to TiCl4. Zr-OTf-EYcatalyzed cross-coupling between THF and 2a was completely shut down in the presence of 1 equiv of TEMPO, indicating the involvement of a radical intermediate in the reaction. Cross-coupling between d_8 -THF and 2a resulted in deuteration in the 2'-position of 3a (Figure S13).

On the basis of these experimental results and literature precedents, ^{15,17} we propose a plausible reaction mechanism for Zr-OTf-EY-catalyzed cross-coupling of THF and **2a** in Figure 4. The strongly Lewis acidic Zr₂-OTf site binds to **2a** to

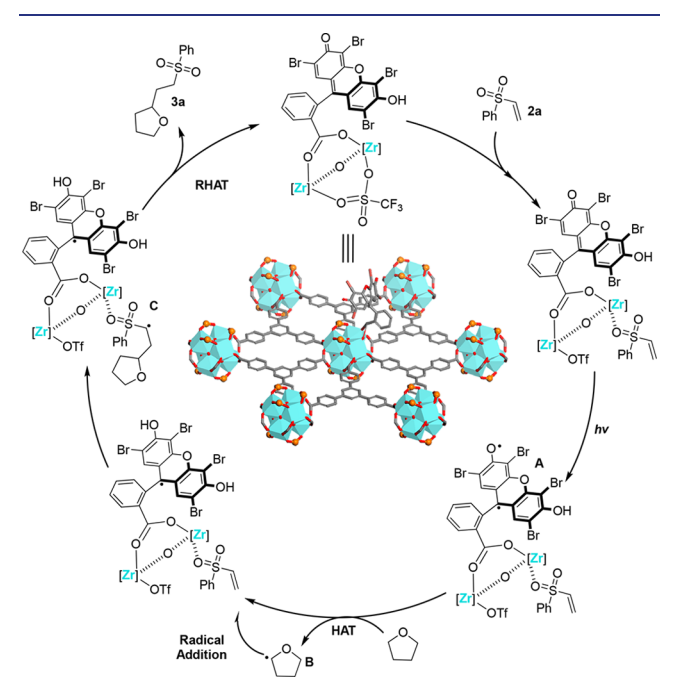


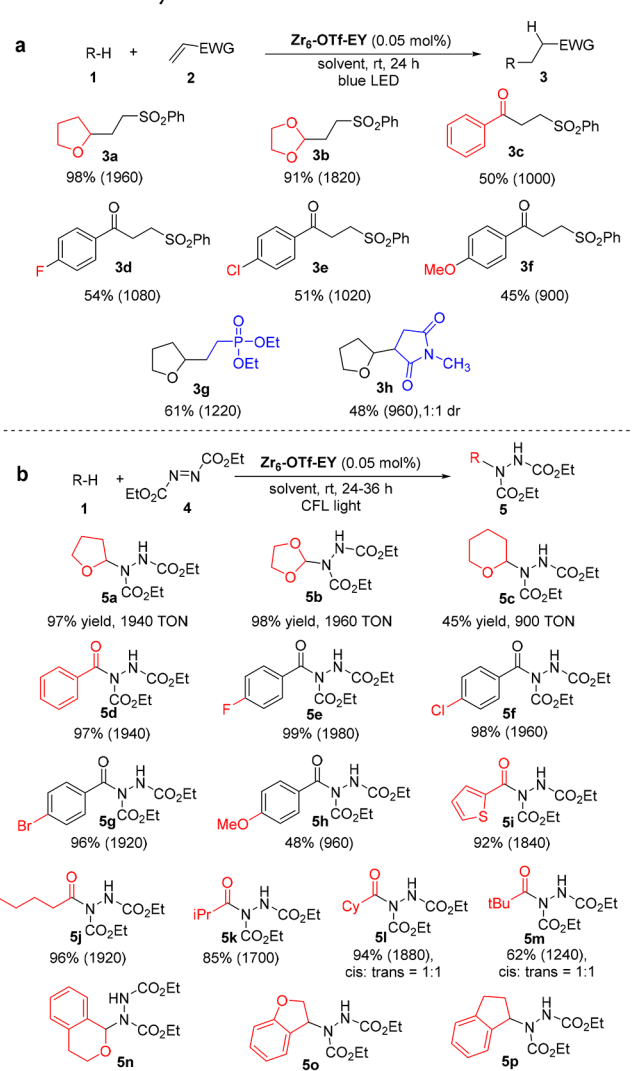
Figure 4. Proposed mechanism for Zr-OTf-EY-catalyzed cross-coupling between THF and 2a.

increase its local concentration near the EY photocatalyst and to enhance its electron deficiency. In the meantime, EY is excited by blue light to form the diradical intermediate A, which undergoes a directed HAT with THF to afford a carbon radical intermediate B. Trapping of B by the activated 2a forms a radical adduct C. A reverse HAT (RHAT) process between C and EY radical affords the product 3a and regenerates EY. In this mechanistic scenario, isolation of EY photocatalysts on the SBUs improves the catalyst stability, which explains the durability of the MOL catalyst in the cross-coupling reactions. Additionally, the proximity between photocatalysts and Lewis acids facilitates the reaction between carbon radical B and activated 2a to enhance the catalytic efficiency by 400 times over the homogeneous control.

We next examined the generality of MOL-based photo-induced HAT. As shown in Table 1a, 0.05 mol % Zr-OTf-EY efficiently catalyzed the cross-coupling of various C-H compounds with electron-deficient alkenes to afford addition products 3. C-H partner 1,3-dioxolane (1b) reacted with 2a to produce Giese adduct 3b in 91% yield with a TON of 1820. Substituents on the benzaldehyde, including hydrogen (1c), fluorine (1d), chlorine (1e), and a methoxy group (1f), were tolerated in the reactions to furnish the corresponding products 3c-3f in 45-54% yields. Other electron-deficient alkenes, diethyl vinylphosphonate (2g) and 1-methyl-1*H*-pyrrole-2,5-dione (2h), coupled with THF to afford alkylation products 3g and 3h in 61% and 48% yield, respectively.

The formation of C-N bonds is one of the most important transformations in organic chemistry and has wide applications in the synthesis of biologically active molecules. ^{50–52} We chose the cross-coupling of diethyl azodicarboxylate (4) with C-H derivatives as a model reaction to evaluate the catalytic

Table 1. Zr-OTf-EY-Catalyzed Cross-Coupling Reactions between C-H Compounds and Electron-Deficient Alkenes or Azodicarboxylate⁴



"Reactions were performed at 0.2 mmol scale with Zr-OTf-EY (0.05—0.1 mol % based on EY) as catalyst at room temperature for 24—36 h. Isolated yield (TON) for each compound.

53% (1060)

60% (1200)

performance of Zr-OTf-EY in C-N bond formation reactions. 53,54 Under CFL light irradiation at room temperature, Zr-OTf-EY (0.05-0.1 mol % based on EY) competently catalyzed the coupling reactions of various C-H derivatives with 4 in good to excellent yields with TONs of up to 1980 (Table 1b). Ethers including tetrahydropyran, 1,3-dioxane, and tetrahydro-2H-pyran afforded addition adducts 5a-5c in 45-98% yields. Aryl-substituted aldehydes with both electronwithdrawing and -donating groups were tolerated to afford the corresponding products 5d-5h in 48-99% isolated yields. Thiophene-2-carbaldehyde also reacted with 4 to afford 5i in 92% yield. The reactions with primary, secondary, and ternary alkyl aldehydes proceeded smoothly to yield products 5i-5m in good to excellent yields. It is worth noting that cis/trans isomers were detected for products 51 and 5m, which contain bulky cyclohexyl and tert-butyl groups. The cross-coupling reactions with benzylic substrates (1n-1p) also proceeded smoothly to afford **5n-5p** in 53-61% yields.

Several control experiments were performed to demonstrate the advantages of Zr-OTf-EY catalyst. Reactions catalyzed by 0.05 mol % EY alone or 0.05 mol % EY and 0.5 mol % Zr-BTB-OTf afforded product 5a in 17% and 36% yield, respectively. Twenty-fold higher loadings of both EY and Zr-BTB-OTf were needed to afford 3a in a comparable yield to Zr-OTf-EY. In addition, the catalytic activity of Zr-BTB-OTf was maintained throughout the reactions, as demonstrated by reuse of Zr-BTB-OTf in four runs of cross-coupling reactions between 2a and 4 with no decrease in the yields of 5a (Figure S11a).

In summary, we have sequentially modified the nodes of Zr-BTB MOL to afford the bifunctional Zr-OTf-EY MOL with strong Lewis acid sites and HAT photocatalysts for hydrofunctionalization reactions. Zr-OTf-EY effectively catalyzed cross-coupling reactions of electron-deficient alkenes or azodicarboxylate with various C-H compounds through photoinduced HAT to afford C-C and C-N bond-forming products with TONs of up to 1980. Zr-OTf-EY outperformed homogeneous controls by 400 times as a result of higher photocatalyst stability, increased local concentrations of Lewis acid-activated alkene and azo substrates, and enhanced alkyl radical transfer from the photocatalyst to the activated substrates. The MOL catalyst was readily recovered and reused in photocatalytic hydrofunctionalization reactions. This work highlights the potential of MOL node modification as an effective strategy for developing synergistic catalysts for sustainable catalysis.

ASSOCIATED CONTENT

Supporting Information

The Supporting Information is available free of charge at https://pubs.acs.org/doi/10.1021/jacs.3c02703.

Materials and methods, synthesis and characterization of Zr-OTf-EY and Zr-OTf-AQ MOLs, catalytic reactions and characterization of products, control experiments, time-dependent study, recycle experiments, Lewis acidity evaluation, and NMR spectra (PDF)

AUTHOR INFORMATION

Corresponding Author

Wenbin Lin — Department of Chemistry, The University of Chicago, Chicago, Illinois 60637, United States;
orcid.org/0000-0001-7035-7759; Email: wenbinlin@uchicago.edu

Authors

Haifeng Zheng – Department of Chemistry, The University of Chicago, Chicago, Illinois 60637, United States

Yingjie Fan − Department of Chemistry, The University of Chicago, Chicago, Illinois 60637, United States;
ocid.org/0000-0003-1857-5788

Abigail L. Blenko – Department of Chemistry, The University of Chicago, Chicago, Illinois 60637, United States

Complete contact information is available at: https://pubs.acs.org/10.1021/jacs.3c02703

Author Contributions

H.Z. and Y.F. contributed equally.

Notes

The authors declare no competing financial interest.

ACKNOWLEDGMENTS

We acknowledge the National Science Foundation (CHE-2102554) and the University of Chicago for funding support and the MRSEC Shared User Facilities at the University of Chicago (DMR-1420709) for instrument access.

REFERENCES

- (1) Capaldo, L.; Ravelli, D.; Fagnoni, M. Direct Photocatalyzed Hydrogen Atom Transfer (HAT) for Aliphatic C-H Bonds Elaboration. *Chem. Rev.* **2022**, *122* (2), 1875–1924.
- (2) Cao, H.; Tang, X.; Tang, H.; Yuan, Y.; Wu, J. Photoinduced intermolecular hydrogen atom transfer reactions in organic synthesis. *Chem. Catal.* **2021**, *1* (3), 523–598.
- (3) Mayer, J. M. Understanding Hydrogen Atom Transfer: From Bond Strengths to Marcus Theory. *Acc. Chem. Res.* **2011**, 44 (1), 36–46
- (4) Capaldo, L.; Ravelli, D. Hydrogen Atom Transfer (HAT): A Versatile Strategy for Substrate Activation in Photocatalyzed Organic Synthesis. *Eur. J. Org. Chem.* **2017**, 2017 (15), 2056–2071.
- (5) Wagner, P. J.; Hammond, G. S. Properties and Reactions of Organic Molecules in their Triplet States. *Adv. Photochem.* **1968**, 21–156.
- (6) Formosinho, S. J. Photochemical hydrogen abstractions as radiationless transitions. Part 2.—Thioketones, quinones, azaaromatics, olefins and azobenzenes. *J. Chem. Soc., Faraday Trans.* 2 1976, 72 (0), 1332–1339.
- (7) Walling, C.; Gibian, M. J. Hydrogen Abstraction Reactions by the Triplet States of Ketones1. *J. Am. Chem. Soc.* **1965**, 87 (15), 3361–3364
- (8) Burrows, H. D.; Formosinho, S. J. Photochemical hydrogen abstractions as radiationless transitions. Part 3.—Theoretical analysis of hydrogen abstraction by excited uranyl (UO) ion. *J. Chem. Soc., Faraday Trans.* 2 1977, 73 (2), 201–208.
- (9) Masakazu, A.; Yutaka, K. Reactivity of Excited Triplet Alkyl Ketones in Solution. I. Quenching and Hydrogen Abstraction of Triplet Acetone. *Bull. Chem. Soc. Jpn.* **1977**, *50* (8), 1913–1916.
- (10) Fan, X.; Zhang, M.; Gao, Y.; Zhou, Q.; Zhang, Y.; Yu, J.; Xu, W.; Yan, J.; Liu, H.; Lei, Z.; Ter, Y. C.; Chanmungkalakul, S.; Lum, Y.; Liu, X.; Cui, G.; Wu, J. Stepwise on-demand functionalization of multihydrosilanes enabled by a hydrogen-atom-transfer photocatalyst based on eosin Y. *Nat. Chem.* **2023**, DOI: 10.1038/s41557-023-01155-8.
- (11) Wu, Y.; Kim, D.; Teets, T. S. Photophysical Properties and Redox Potentials of Photosensitizers for Organic Photoredox Transformations. *Synlett* **2021**, *33* (12), 1154–1179.
- (12) Wagner, P. J.; Truman, R. J.; Scaiano, J. C. Substituent effects on hydrogen abstraction by phenyl ketone triplets. *J. Am. Chem. Soc.* **1985**, *107* (24), 7093–7097.
- (13) Chandra, A. K. The perturbational treatment of the process of hydrogen abstraction by ketones. *J. Photochem.* **1979**, *11* (5), 347–360.
- (14) Péter, Á.; Agasti, S.; Knowles, O.; Pye, E.; Procter, D. J. Recent advances in the chemistry of ketyl radicals. *Chem. Soc. Rev.* **2021**, *50* (9), 5349–5365.
- (15) Luo, Y.; Wei, Q.; Yang, L.; Zhou, Y.; Cao, W.; Su, Z.; Liu, X.; Feng, X. Enantioselective Radical Hydroacylation of α,β -Unsaturated Carbonyl Compounds with Aldehydes by Triplet Excited Anthraquinone. *ACS Catal.* **2022**, *12* (20), 12984–12992.
- (16) Dai, Z.-Y.; Nong, Z.-S.; Wang, P.-S. Light-Mediated Asymmetric Aliphatic C-H Alkylation with Hydrogen Atom Transfer Catalyst and Chiral Phosphoric Acid. *ACS Catal.* **2020**, *10* (8), 4786–4790
- (17) Kuang, Y.; Wang, K.; Shi, X.; Huang, X.; Meggers, E.; Wu, J. Asymmetric Synthesis of 1,4-Dicarbonyl Compounds from Aldehydes by Hydrogen Atom Transfer Photocatalysis and Chiral Lewis Acid Catalysis. *Angew. Chem., Int. Ed.* **2019**, *58* (47), 16859–16863.
- (18) Cardarelli, A. M.; Fagnoni, M.; Mella, M.; Albini, A. Hydrocarbon Activation. Synthesis of β -Cycloalkyl (Di)nitriles

- through Photosensitized Conjugate Radical Addition. J. Org. Chem. 2001, 66 (22), 7320-7327.
- (19) Zhou, M.-J.; Zhang, L.; Liu, G.; Xu, C.; Huang, Z. Site-Selective Acceptorless Dehydrogenation of Aliphatics Enabled by Organo-photoredox/Cobalt Dual Catalysis. *J. Am. Chem. Soc.* **2021**, *143* (40), 16470–16485.
- (20) Huo, H.; Shen, X.; Wang, C.; Zhang, L.; Röse, P.; Chen, L.-A.; Harms, K.; Marsch, M.; Hilt, G.; Meggers, E. Asymmetric photoredox transition-metal catalysis activated by visible light. *Nature* **2014**, *515* (7525), 100–103.
- (21) Drake, T.; Ji, P.; Lin, W. Site Isolation in Metal-Organic Frameworks Enables Novel Transition Metal Catalysis. *Acc. Chem. Res.* **2018**, *51* (9), 2129–2138.
- (22) Feng, X.; Song, Y.; Li, Z.; Kaufmann, M.; Pi, Y.; Chen, J. S.; Xu, Z.; Li, Z.; Wang, C.; Lin, W. Metal-Organic Framework Stabilizes a Low-Coordinate Iridium Complex for Catalytic Methane Borylation. *J. Am. Chem. Soc.* **2019**, *141* (28), 11196–11203.
- (23) Sawano, T.; Lin, Z.; Boures, D.; An, B.; Wang, C.; Lin, W. Metal-Organic Frameworks Stabilize Mono(phosphine)-Metal Complexes for Broad-Scope Catalytic Reactions. *J. Am. Chem. Soc.* **2016**, 138 (31), 9783–9786.
- (24) Lv, X.-L.; Wang, K.; Wang, B.; Su, J.; Zou, X.; Xie, Y.; Li, J.-R.; Zhou, H.-C. A Base-Resistant Metalloporphyrin Metal-Organic Framework for C-H Bond Halogenation. *J. Am. Chem. Soc.* **2017**, 139 (1), 211–217.
- (25) Wang, Z.; Zeng, L.; He, C.; Duan, C. Metal-Organic Framework-Encapsulated Anthraquinone for Efficient Photocatalytic Hydrogen Atom Transfer. *ACS Appl. Mater. Interfaces* **2022**, *14* (6), 7980–7989.
- (26) Cao, C.-C.; Chen, C.-X.; Wei, Z.-W.; Qiu, Q.-F.; Zhu, N.-X.; Xiong, Y.-Y.; Jiang, J.-J.; Wang, D.; Su, C.-Y. Catalysis through Dynamic Spacer Installation of Multivariate Functionalities in Metal-Organic Frameworks. *J. Am. Chem. Soc.* **2019**, *141* (6), 2589–2593.
- (27) Hwang, Y. K.; Hong, D.-Y.; Chang, J.-S.; Jhung, S. H.; Seo, Y.-K.; Kim, J.; Vimont, A.; Daturi, M.; Serre, C.; Férey, G. Amine Grafting on Coordinatively Unsaturated Metal Centers of MOFs: Consequences for Catalysis and Metal Encapsulation. *Angew. Chem., Int. Ed.* 2008, 47 (22), 4144–4148.
- (28) Yuan, S.; Chen, Y.-P.; Qin, J.-S.; Lu, W.; Zou, L.; Zhang, Q.; Wang, X.; Sun, X.; Zhou, H.-C. Linker Installation: Engineering Pore Environment with Precisely Placed Functionalities in Zirconium MOFs. J. Am. Chem. Soc. 2016, 138 (28), 8912–8919.
- (29) Chang, G.-G.; Ma, X.-C.; Zhang, Y.-X.; Wang, L.-Y.; Tian, G.; Liu, J.-W.; Wu, J.; Hu, Z.-Y.; Yang, X.-Y.; Chen, B. Construction of Hierarchical Metal-Organic Frameworks by Competitive Coordination Strategy for Highly Efficient CO2 Conversion. *Adv. Mater.* **2019**, 31 (52), 1904969.
- (30) Zhou, W.; Huang, D.-D.; Wu, Y.-P.; Zhao, J.; Wu, T.; Zhang, J.; Li, D.-S.; Sun, C.; Feng, P.; Bu, X. Stable Hierarchical Bimetal-Organic Nanostructures as HighPerformance Electrocatalysts for the Oxygen Evolution Reaction. *Angew. Chem., Int. Ed.* **2019**, 58 (13), 4227–4231.
- (31) Wang, Y.; Jia, X.; Yang, H.; Wang, Y.; Chen, X.; Hong, A. N.; Li, J.; Bu, X.; Feng, P. A Strategy for Constructing Pore-Space-Partitioned MOFs with High Uptake Capacity for C2 Hydrocarbons and CO2. *Angew. Chem., Int. Ed.* **2020**, *59* (43), 19027–19030.
- (32) Niu, Z.; Zhang, W.; Lan, P. C.; Aguila, B.; Ma, S. Promoting Frustrated Lewis Pairs for Heterogeneous Chemoselective Hydrogenation via the Tailored Pore Environment within Metal-Organic Frameworks. *Angew. Chem., Int. Ed.* **2019**, 58 (22), 7420–7424.
- (33) Chen, C.-X.; Wei, Z.-W.; Pham, T.; Lan, P. C.; Zhang, L.; Forrest, K. A.; Chen, S.; Al-Enizi, A. M.; Nafady, A.; Su, C.-Y.; Ma, S. Nanospace Engineering of Metal-Organic Frameworks through Dynamic Spacer Installation of Multifunctionalities for Efficient Separation of Ethane from Ethane/Ethylene Mixtures. *Angew. Chem., Int. Ed.* **2021**, *60* (17), 9680–9685.
- (34) Lan, G.; Fan, Y.; Shi, W.; You, E.; Veroneau, S. S.; Lin, W. Biomimetic active sites on monolayered metal-organic frameworks for artificial photosynthesis. *Nat. Catal.* **2022**, *5* (11), 1006–1018.

- (35) Zheng, H.; Fan, Y.; Song, Y.; Chen, J. S.; You, E.; Labalme, S.; Lin, W. Site Isolation in Metal-Organic Layers Enhances Photoredox Gold Catalysis. *J. Am. Chem. Soc.* **2022**, *144* (24), 10694–10699.
- (36) Fan, Y.; You, E.; Xu, Z.; Lin, W. A Substrate-Binding Metal-Organic Layer Selectively Catalyzes Photoredox Ene-Carbonyl Reductive Coupling Reactions. *J. Am. Chem. Soc.* **2021**, *143* (45), 18871–18876.
- (37) Quan, Y.; Shi, W.; Song, Y.; Jiang, X.; Wang, C.; Lin, W. Bifunctional Metal-Organic Layer with Organic Dyes and Iron Centers for Synergistic Photoredox Catalysis. *J. Am. Chem. Soc.* **2021**, *143* (8), 3075–3080.
- (38) Feng, X.; Song, Y.; Lin, W. Dimensional Reduction of Lewis Acidic Metal-Organic Frameworks for Multicomponent Reactions. *J. Am. Chem. Soc.* **2021**, *143* (21), 8184–8192.
- (39) Quan, Y.; Lan, G.; Fan, Y.; Shi, W.; You, E.; Lin, W. Metal-Organic Layers for Synergistic Lewis Acid and Photoredox Catalysis. *J. Am. Chem. Soc.* **2020**, *142* (4), 1746–1751.
- (40) Feng, X.; Song, Y.; Lin, W. Transforming Hydroxide-Containing Metal-Organic Framework Nodes for Transition Metal Catalysis. *Trends Chem.* **2020**, 2 (11), 965–979.
- (41) Wang, R.; Wang, Z.; Xu, Y.; Dai, F.; Zhang, L.; Sun, D. Porous Zirconium Metal-Organic Framework Constructed from $2D \rightarrow 3D$ Interpenetration Based on a 3,6-Connected kgd Net. *Inorg. Chem.* **2014**, 53 (14), 7086–7088.
- (42) Tao, Z.-R.; Wu, J.-X.; Zhao, Y.-J.; Xu, M.; Tang, W.-Q.; Zhang, Q.-H.; Gu, L.; Liu, D.-H.; Gu, Z.-Y. Untwisted restacking of two-dimensional metal-organic framework nanosheets for highly selective isomer separations. *Nat. Commun.* **2019**, *10* (1), 2911.
- (43) Qiao, G.-Y.; Yuan, S.; Pang, J.; Rao, H.; Lollar, C. T.; Dang, D.; Qin, J.-S.; Zhou, H.-C.; Yu, J. Functionalization of Zirconium-Based Metal-Organic Layers with Tailored Pore Environments for Heterogeneous Catalysis. *Angew. Chem., Int. Ed.* **2020**, *59* (41), 18224–18228.
- (44) Feng, L.; Qiu, Y.; Guo, Q.-H.; Chen, Z.; Seale, J. S. W.; He, K.; Wu, H.; Feng, Y.; Farha, O. K.; Astumian, R. D.; Stoddart, J. F. Active mechanisorption driven by pumping cassettes. *Science* **2021**, *374* (6572), 1215–1221.
- (45) Raviola, C.; Ravelli, D. Efficiency and Selectivity Aspects in the C-H Functionalization of Aliphatic Oxygen Heterocycles by Photocatalytic Hydrogen Atom Transfer. *Synlett* **2019**, *30* (07), 803–808.
- (46) Zhang, Y.; Yang, X.; Wu, J.; Huang, D. Aerobic C-H Functionalization Using Pyrenedione as the Photocatalyst. *Synthesis* **2020**, 52 (17), 2512–2520.
- (47) Kamijo, S.; Takao, G.; Kamijo, K.; Tsuno, T.; Ishiguro, K.; Murafuji, T. Alkylation of Nonacidic C(sp3)-H Bonds by Photo-induced Catalytic Michael-Type Radical Addition. *Org. Lett.* **2016**, *18* (19), 4912–4915.
- (48) Fan, X.-Z.; Rong, J.-W.; Wu, H.-L.; Zhou, Q.; Deng, H.-P.; Tan, J. D.; Xue, C.-W.; Wu, L.-Z.; Tao, H.-R.; Wu, J. Eosin Y as a Direct Hydrogen-Atom Transfer Photocatalyst for the Functionalization of C-H Bonds. *Angew. Chem., Int. Ed.* **2018**, *57* (28), 8514–8518.
- (49) Ji, P.; Drake, T.; Murakami, A.; Oliveres, P.; Skone, J. H.; Lin, W. Tuning Lewis Acidity of Metal-Organic Frameworks via Perfluorination of Bridging Ligands: Spectroscopic, Theoretical, and Catalytic Studies. J. Am. Chem. Soc. 2018, 140 (33), 10553–10561.
- (50) Bariwal, J.; Van der Eycken, E. C-N bond forming cross-coupling reactions: an overview. *Chem. Soc. Rev.* **2013**, 42 (24), 9283–9303.
- (51) Song, G.; Wang, F.; Li, X. C-C, C-O and C-N bond formation via rhodium(iii)-catalyzed oxidative C-H activation. *Chem. Soc. Rev.* **2012**, *41* (9), 3651–3678.
- (52) Lundgren, R. J.; Wilsily, A.; Marion, N.; Ma, C.; Chung, Y. K.; Fu, G. C. Catalytic Asymmetric C-N Bond Formation: Phosphine-Catalyzed Intra- and Intermolecular γ -Addition of Nitrogen Nucleophiles to Allenoates and Alkynoates. *Angew. Chem., Int. Ed.* **2013**, 52 (9), 2525–2528.
- (53) Zhang, H.-B.; Wang, Y.; Gu, Y.; Xu, P.-F. Lewis- and Brønsted-acid cooperative catalytic radical coupling of aldehydes and azodicarboxylate. *RSC Adv.* **2014**, *4* (53), 27796–27799.

(54) Papadopoulos, G. N.; Kokotos, C. G. Photoorganocatalytic One-Pot Synthesis of Hydroxamic Acids from Aldehydes. *Chem.—Eur. J.* **2016**, 22 (20), 6964–6967.